Observation of $\psi(3770) \to \gamma\chi_{c0}$*

R. A. Briere,[1] I. Brock,[1] J. Chen,[1] T. Ferguson,[1] G. Tatishvili,[1] H. Vogel,[1] M. E. Watkins,[1] J. L. Rosner,[2] N. E. Adam,[3] J. P. Alexander,[3] K. Berkelman,[3] D. G. Cassel,[3] J. E. Duboscq,[3] K. M. Ecklund,[3] R. Ehrlich,[3] L. Fields,[3] R. S. Galik,[3] L. Gibbons,[3] R. Gray,[3] S. W. Gray,[3] D. L. Hartill,[3] B. K. Heltsley,[3] D. Hertz,[3] C. D. Jones,[3] J. Kandaswamy,[3] D. L. Kreinick,[3] V. E. Kuznetsov,[3] H. Mahlke-Krüger,[3] T. O. Meyer,[3] P. U. E. Onyisi,[3] J. R. Patterson,[3] D. Peterson,[3] J. Pivarski,[3] D. Riley,[3] A. Ryd,[3] A. J. Sadoff,[3] H. Schwarthoff,[3] X. Shi,[3] S. Stroiney,[3] W. M. Sun,[3] T. Wilksen,[3] M. Weinberger,[3] S. B. Athar,[4] R. Patel,[4] V. Potlia,[4] H. Stoeck,[4] J. Yelton,[4] P. Rubin,[5] C. Cawlfield,[6] B. I. Eisenstein,[6] I. Karliner,[6] D. Kim,[6] N. Lowrey,[6] P. Naik,[6] C. Sedlack,[6] M. Selen,[6] E. J. White,[6] J. Wiss,[6] M. R. Shepherd,[7] D. Besson,[8] T. K. Pedlar,[9] D. Cronin-Hennessy,[10] K. Y. Gao,[10] D. T. Gong,[10] J. Hietala,[10] Y. Kubota,[10] T. Klein,[10] B. W. Lang,[10] R. Poling,[10] A. W. Scott,[10] A. Smith,[10] S. Dobbs,[11] Z. Metreveli,[11] K. K. Seth,[11] A. Tomaradze,[11] P. Zweber,[11] J. Ernst,[12] H. Severini,[13] S. A. Dytman,[14] W. Love,[14] V. Savinov,[14] O. Aquines,[15] Z. Li,[15] A. Lopez,[15] S. Mehrabyan,[15] H. Mendez,[15] J. Ramirez,[15] G. S. Huang,[16] D. H. Miller,[16] V. Pavlunin,[16] B. Sanghi,[16] I. P. J. Shipsey,[16] B. Xin,[16] G. S. Adams,[17] M. Anderson,[17] J. P. Cummings,[17] I. Danko,[17] J. Napolitano,[17] Q. He,[18] J. Insler,[18] H. Muramatsu,[18] C. S. Park,[18] E. H. Thorndike,[18] T. E. Coan,[19] Y. S. Gao,[19] F. Liu,[19] M. Artuso,[20] S. Blusk,[20] J. Butt,[20] J. Li,[20] N. Menaa,[20] R. Mountain,[20] S. Nisar,[20] K. Randrianarivony,[20] R. Redjimi,[20] R. Sia,[20] T. Skwarnicki,[20] S. Stone,[20] J. C. Wang,[20] K. Zhang,[20] S. E. Csorna,[21] G. Bonvicini,[22] D. Cinabro,[22] M. Dubrovin,[22] A. Lincoln,[22] D. M. Asner,[23] and K. W. Edwards[23]

(CLEO Collaboration)

[1]*Carnegie Mellon University, Pittsburgh, Pennsylvania 15213*
[2]*Enrico Fermi Institute, University of Chicago, Chicago, Illinois 60637*
[3]*Cornell University, Ithaca, New York 14853*
[4]*University of Florida, Gainesville, Florida 32611*
[5]*George Mason University, Fairfax, Virginia 22030*
[6]*University of Illinois, Urbana-Champaign, Illinois 61801*
[7]*Indiana University, Bloomington, Indiana 47405*
[8]*University of Kansas, Lawrence, Kansas 66045*
[9]*Luther College, Decorah, Iowa 52101*
[10]*University of Minnesota, Minneapolis, Minnesota 55455*
[11]*Northwestern University, Evanston, Illinois 60208*
[12]*State University of New York at Albany, Albany, New York 12222*
[13]*University of Oklahoma, Norman, Oklahoma 73019*
[14]*University of Pittsburgh, Pittsburgh, Pennsylvania 15260*
[15]*University of Puerto Rico, Mayaguez, Puerto Rico 00681*
[16]*Purdue University, West Lafayette, Indiana 47907*
[17]*Rensselaer Polytechnic Institute, Troy, New York 12180*
[18]*University of Rochester, Rochester, New York 14627*
[19]*Southern Methodist University, Dallas, Texas 75275*
[20]*Syracuse University, Syracuse, New York 13244*
[21]*Vanderbilt University, Nashville, Tennessee 37235*

[22] *Wayne State University, Detroit, Michigan 48202*
[23] *Carleton University, Ottawa, Ontario, Canada K1S 5B6*
(Dated: July 23, 2006)

Abstract

From e^+e^- collision data acquired with the CLEO-c detector at CESR, we search for the non-$D\bar{D}$ decays $\psi(3770) \to \gamma\chi_{cJ}$, with χ_{cJ} reconstructed in four exclusive decays modes containing charged pions and kaons. We report the first observation of such decays for $J = 0$ with a branching ratio of $(0.73 \pm 0.07 \pm 0.06)\%$. The rates for different J are consistent with the expectations assuming $\psi(3770)$ is predominantly a 1^3D_1 state of charmonium, but only if relativistic corrections are applied.

*Submitted to the 33rd International Conference on High Energy Physics, July 26 - August 2, 2006, Moscow

Observation of the narrow $X(3872)$ and $Y(4260)$ states [1] above open charm threshold, and their possible interpretation as states beyond the traditional $c\bar{c}$ model of charmonium [2], calls for thorough investigation of the lightest charmonium state above the $D\bar{D}$ threshold - $\psi(3770)$. The common interpretation of the $\psi(3770)$ assumes it is predominantly the 1^3D_1 $c\bar{c}$ state, with a small admixture of 2^3S_1. Except for the large $D\bar{D}$ decay width and rough agreement with the potential model mass predictions, there have been no other experimental data to verify this assumption. Although decays of $\psi(3770)$ to $\pi^+\pi^- J/\psi$, $\pi^0\pi^0 J/\psi$ and $\eta J/\psi$ have been measured to be non-zero [3, 4], such hadronic modes present a less sensitive probe of the charmonium model than rates for $\psi(3770) \to \gamma\chi_{cJ}$ since they involve hadronization probabilities.

Previously, we have reported observation of $\psi(3770) \to \gamma\chi_{c1}$ with $\chi_{c1} \to \gamma J/\psi$, $J/\psi \to l^+l^-$ [5]. The branching ratio for $\psi(3770) \to \gamma\chi_{c0}$ is predicted to be the largest [6–9], but the small branching ratio for $\chi_{c0} \to \gamma J/\psi$ reduces the sensitivity so much that only a loose upper limit could be set in Ref. [5]. However, hadronic χ_{c0} decays are copious and thereby offer complementary probes for these photon transitions. Backgrounds from $D\bar{D}$ decays and continuum processes are suppressed by full reconstruction of χ_{cJ} decays to a few exclusive hadronic final states. We use the following decay modes: $\chi_{cJ} \to K^+K^-$ $(2K)$, $\chi_{cJ} \to \pi^+\pi^-\pi^+\pi^-$ (4π), $\chi_{cJ} \to K^+K^-\pi^+\pi^-$ $(2K2\pi)$ and $\chi_{cJ} \to \pi^+\pi^-\pi^+\pi^-\pi^+\pi^-$ (6π). To minimize sensitivity to large uncertainties in branching fractions and resonant substructure for these channels, we measure the rates relative to those seen in $\psi(2S)$ decays with the same detector,

$$R_J \equiv \frac{\mathcal{B}(\psi(3770) \to \gamma\chi_{cJ}) \times \mathcal{B}(\chi_{cJ} \to \pi^\pm, K^\pm)}{\mathcal{B}(\psi(2S) \to \gamma\chi_{cJ}) \times \mathcal{B}(\chi_{cJ} \to \pi^\pm, K^\pm)},$$

and normalize to $\mathcal{B}(\psi(2S) \to \gamma\chi_{cJ})$ [10], which was measured by fitting inclusive photon energy spectra. Thus, our results for $\mathcal{B}(\psi(3770) \to \gamma\chi_{cJ})$ are not only independent of $\mathcal{B}(\chi_{cJ} \to \pi^\pm, K^\pm)$, but also depend only on ratios of detection efficiencies for $\psi(3770)$ and $\psi(2S)$. The latter are almost independent of the resonant substructure and, therefore, can be more reliably determined.

The data were acquired at a center-of-mass energy of 3773 MeV with the CLEO-c detector [11] operating at the Cornell Electron Storage Ring (CESR), and correspond to an integrated luminosity (number of resonant decays) of 281 pb^{-1} ($(1.80 \pm 0.05) \times 10^6$) at the $\psi(3770)$ and 2.9 pb^{-1} ($(1.51 \pm 0.05) \times 10^6$) at the $\psi(2S)$. The CLEO-c detector features a solid angle coverage of 93% for charged and neutral particles. The cesium iodide (CsI) calorimeter attains photon energy resolutions of 2.2% at $E_\gamma = 1$ GeV and 5% at 100 MeV. For the data presented here, the charged particle tracking system operates in a 1.0 T magnetic field along the beam axis and achieves a momentum resolution of 0.6% at p = 1 GeV. Particle identification is performed using Ring-Imaging Cherenkov Detector (RICH) in combination with specific ionization loss (dE/dx) in the gaseous tracking volume.

We select events with exactly 6, 4 or 2 charged tracks and at least one photon candidate with energy above 60 MeV. The highest energy photon is considered to be the signal photon, while other neutral clusters in the calorimeter are considered fragments of hadronic showers, and therefore ignored. We separate pions and kaons using a log-likelihood difference, which optimally combines the dE/dX and RICH information. The track is considered a kaon if the kaon hypothesis is more likely. The RICH information is used only if the track momentum is above kaon radiation threshold (700 MeV) and the number of Cherenkov photons for the kaon hypothesis is required to be at least 3 in this case. We also impose 3σ consistency on dE/dx. Those tracks not identified as kaons become pion candidates if they satisfy 3σ

TABLE I: Efficiencies for $\psi(2S)/\psi(3770) \to \gamma\chi_{cJ}$, $\chi_{cJ} \to \pi^{\pm}, K^{\pm}$, based on Monte Carlo of phase-space χ_{cJ} decays (i.e. no intermediate resonances).

		Efficiency (%)		
		$J=2$	$J=1$	$J=0$
$\psi(2S) \to \gamma\chi_{cJ} \to$	4π	33	35	34
	$2K2\pi$	25	27	28
	6π	23	25	27
	$2K$	43	44	42
$\psi(3770) \to \gamma\chi_{cJ} \to$	4π	35	36	34
	$2K2\pi$	29	30	29
	6π	27	28	27
	$2K$	44	44	41

consistency with dE/dX. Events with odd numbers of kaons or pions are rejected. The total energy and Cartesian components of momentum of the selected charged particles and the photon must be consistent within ± 30 MeV with the expected center-of-mass four-vector components, which take into account a small beam crossing angle. To improve resolution on the photon energy, we then constrain these quantities to the expected values via kinematic fitting of events. Selection efficiencies obtained with GEANT [12] based simulation of detector response are given in Table I.

The energy of the photon candidates is plotted for the data for different decay channels in Fig. 1 and Fig. 2. Fits used to extract signal amplitudes are also shown. Each photon line is represented by a detector response function, parameterized by the so-called Crystal Ball line (CBL) shape. CBL is a Gaussian (described by the peak energy, E_0, and energy resolution, σ_E) turning into a power law tail, $1/(E_0 - E + \text{const})^n$, at an energy of $E_0 - \alpha\sigma_E$. We fix α and n to the values determined from the signal Monte Carlo. The peak amplitude ($A^{\text{in } \psi(2S)}_{\psi(2S)}$), peak energy and widths are free parameters in the fit to the $\psi(2S)$ data. The smooth background is represented by a first order polynomial. In the fit to the $\psi(3770)$ data only the peak amplitudes ($A_{\psi(3770)}$) are free parameters, while the CBL parameters are fixed to the predictions from the signal Monte Carlo. In addition to the smooth backgrounds, represented by a second order polynomial, the $\psi(3770)$ data also contain radiatively produced $\psi(2S)$ background. After our selection cuts, the latter cannot be distinguished from the $\psi(3770)$ signal. They are explicitly represented in the fit by peaks with the amplitudes, $A^{\text{in } \psi(3770)}_{\psi(2S)}$, fixed to the values estimated from the $\psi(2S)$ data ($A^{\text{in } \psi(2S)}_{\psi(2S)}$) and extrapolated to the $\psi(3770)$ beam energy with help of the theoretical formulae:

$$A^{\text{in } \psi(3770)}_{\psi(2S)} = \mathcal{L}_{\psi(3770)} \cdot \epsilon_{\psi(3770)} \cdot \mathcal{B}_X \cdot \Gamma_{ee}(\psi(2S)) \cdot I(s)$$

$$I(s) = \int_0^{x_{cut}} W(s,x) \cdot b(s'(x)) \cdot F_X(s'(x)) dx.$$

Here, we are using the same notation as in Ref. [4]: $\mathcal{L}$ is the integrated luminosity; ϵ is the efficiency; $\mathcal{B}_X$ is the branching ratio for $\psi(2S) \to \gamma\chi_{cJ} \to \gamma X$ (X is the hadronic final state) at the $\psi(2S)$ resonance peak; x is energy radiated in $e^+e^- \to \gamma\psi(2S)$ divided by its maximal possible value (i.e. by $E_{\text{beam}} = \sqrt{s}/2$); s' is the mass-squared with which the $\psi(2S)$

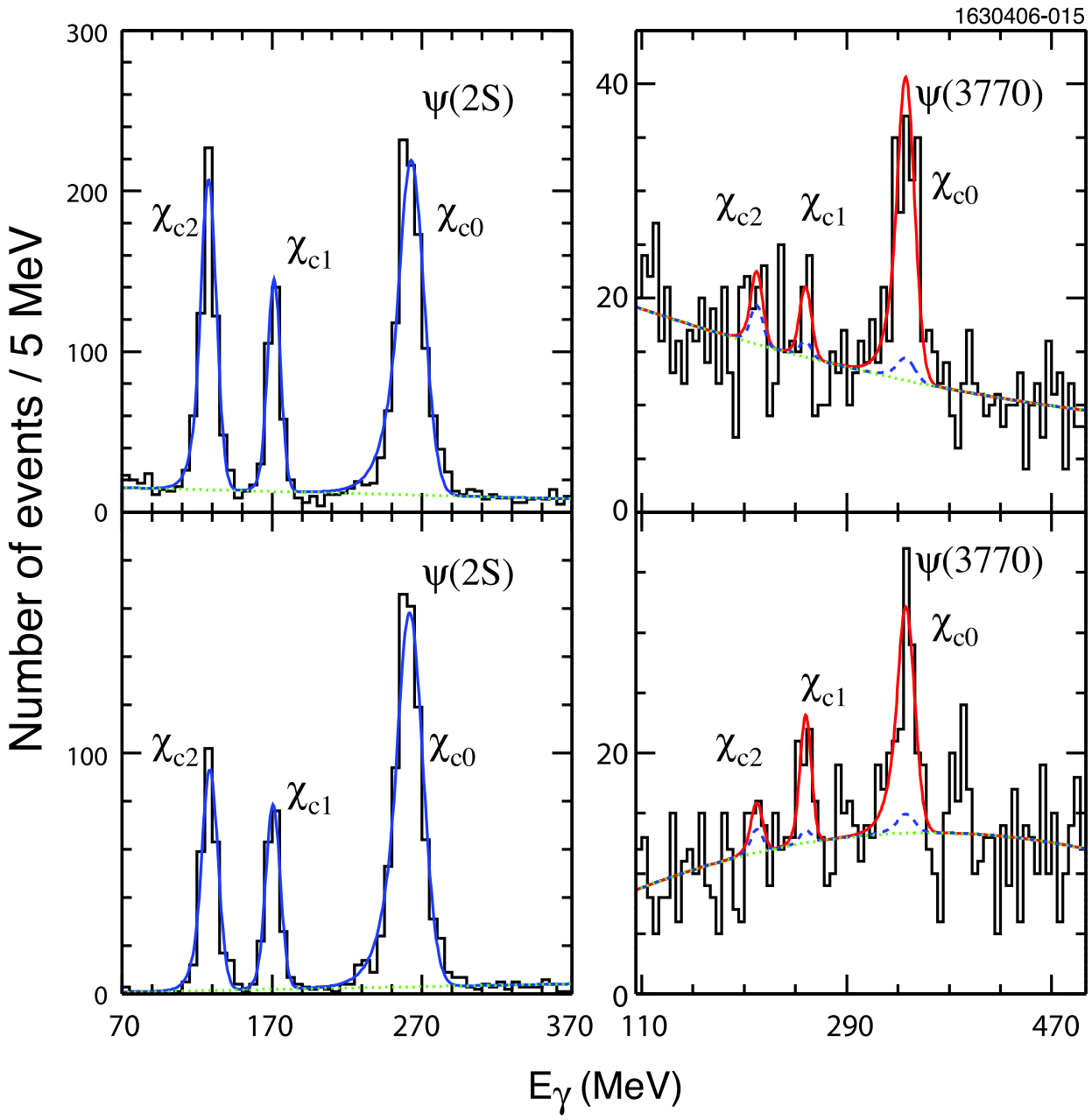

FIG. 1: Distribution of photon energy for 4π (top) and $2K2\pi$ (bottom) decay samples in CLEO-c $\psi(2S)$ (left) and $\psi(3770)$ (right) data. Solid histogram is data, smooth curve is fit to the data. Dashed line shows radiative return background contribution from $\psi(2S)$ tail and dotted line is polynomial background.

is produced ($s'(x) = s(1-x)$); $W(s,x)$ is the initial state radiation probability (see Ref. [4] for the definition and discussion); $b(s')$ is the relativistic Breit-Wigner formula describing the $\psi(2S)$ resonance ($b(s') = 12\pi\Gamma_R/[(s'-M_R^2)^2 + M_R^2\Gamma_R^2]$); and $F_X(s')$ is the phase-space factor between the $\psi(2S)$ produced with $\sqrt{s'}$ mass and with its nominal mass, M_R. $F_X(s')$ is equal [13] to $(E_\gamma(s')/E_\gamma(M_R^2))^3$, where E_γ is the photon energy in $\psi(2S) \to \gamma\chi_{cJ}$ decay. The $\psi(2S)$ nominal mass (M_R) and total width (Γ_R) are taken from PDG [14], while $\Gamma_{ee}(\psi(2S))$

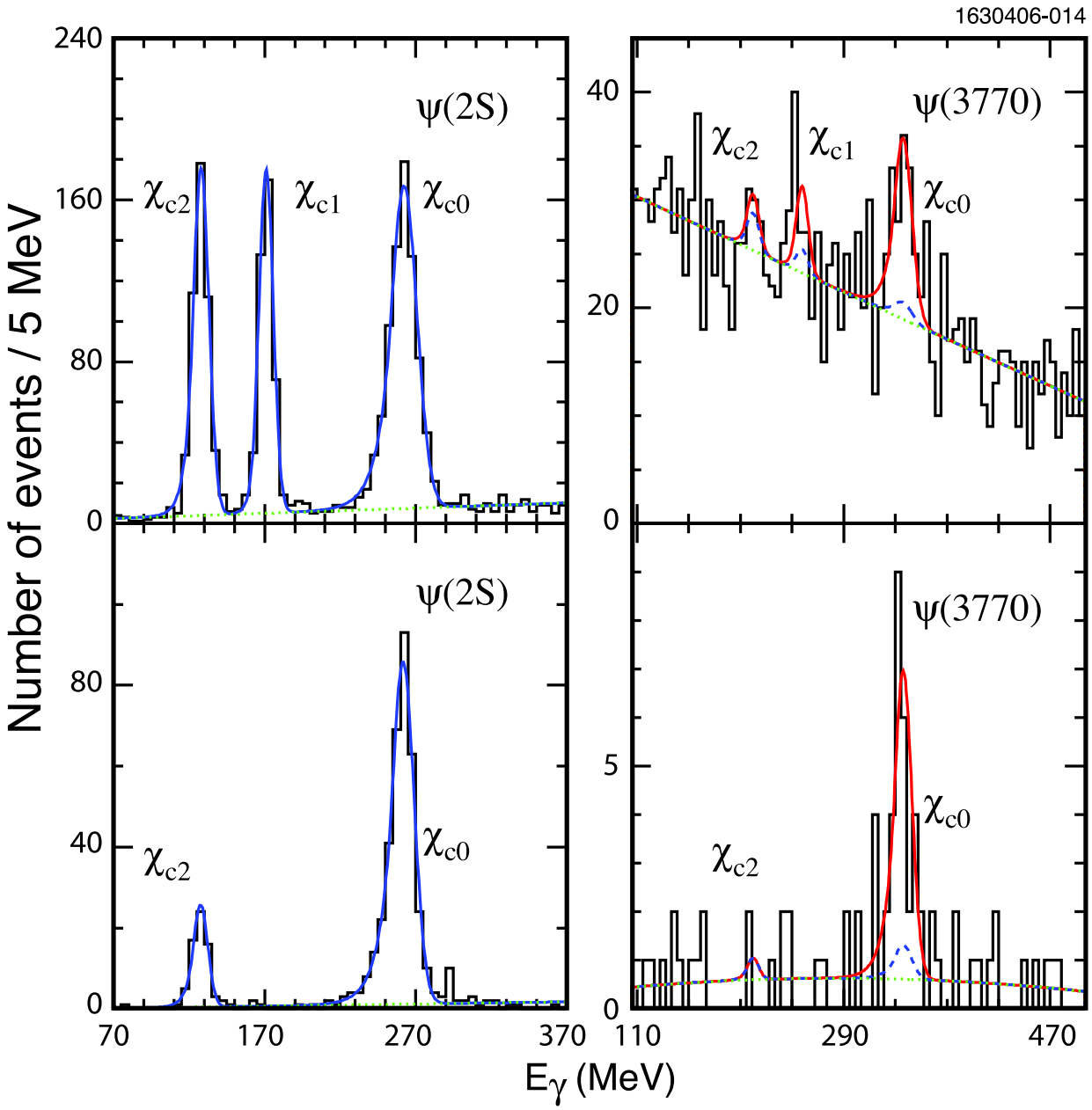

FIG. 2: Distribution of photon energy for 6π (top) and $2K$ (bottom) decay samples in CLEO-c $\psi(2S)$ (left) and $\psi(3770)$ (right) data. Solid histogram is data, smooth curve is fit to the data. Dashed line shows radiative return background contribution from $\psi(2S)$ tail and dotted line is polynomial background.

is taken from the CLEO determination utilizing $e^+e^- \to \gamma\psi(2S)$ at $E_{CM} = 3773$ MeV with $\psi(2S)$ decaying to J/ψ through a hadronic transition [4]. The radiative flux, $W(s,x)$, strongly peaks for $x \to 0$ making the $\psi(2S)$ background indistinguishable from the $\psi(3770)$ signal within our photon energy resolution. Unlike in our $X = \gamma J/\psi$ analysis [5], where we used the published CLEO results for $\mathcal{B}_X$ and relied on the absolute value of the detection

TABLE II: Fitted signal yields for $\psi(2S)/\psi(3770) \to \gamma\chi_{cJ}$, $\chi_{cJ} \to \pi^{\pm}, K^{\pm}$. The total number of the estimated $\psi(2S)$ background events in the $\psi(3770)$ data ($A^{\text{in }\psi(3770)}_{\psi(2S)}$) is also given. The errors on the latter quantities are systematic. All other errors are statistical.

	Decay	Events		
	Mode	$J=2$	$J=1$	$J=0$
$A^{\text{in }\psi(2S)}_{\psi(2S)}$	4π	534 ± 27	291 ± 19	981 ± 36
	$2K2\pi$	261 ± 16	187 ± 14	745 ± 29
	6π	469 ± 23	408 ± 21	744 ± 30
	$2K$	64 ± 8	–	346 ± 19
	All	1329 ± 40	886 ± 32	2816 ± 58
$A^{\text{in }\psi(3770)}_{\psi(2S)}$	All	25 ± 6	12 ± 3	25 ± 6
$A_{\psi(3770)}$	4π	9 ± 10	14 ± 9	112 ± 16
	$2K2\pi$	6 ± 8	25 ± 9	73 ± 14
	6π	5 ± 12	16 ± 11	65 ± 16
	$2K$	0 ± 1	–	24 ± 6
	All	20 ± 18	54 ± 17	274 ± 27

efficiency ($\epsilon_{\psi}(3770)$), in this analysis we set

$$\mathcal{B}_X = \frac{A^{\text{in }\psi(2S)}_{\psi(2S)}}{\epsilon_{\psi(2S)} \cdot N_{\psi(2S)}},$$

where $A^{\text{in }\psi(2S)}_{\psi(2S)}$ is the signal yield in the fit to the $\psi(2S)$ data. Therefore, our estimates of the $\psi(2S)$ radiative tail background,

$$A^{\text{in }\psi(3770)}_{\psi(2S)} = A^{\text{in }\psi(2S)}_{\psi(2S)} \cdot \frac{\epsilon_{\psi(3770)}}{\epsilon_{\psi(2S)}} \cdot \frac{\mathcal{L}_{\psi(3770)}}{N_{\psi(2S)}} \cdot \Gamma_{ee}(\psi(2S)) \cdot I(s),$$

do not rely on absolute values of efficiencies, but only on their ratio between the $\psi(3770)$ and $\psi(2S)$ data samples. The upper range of integration in the definition of $I(s)$ is $x_{\text{cut}} \approx 30$ MeV/1887 MeV=0.016, because of our cuts on total energy and momentum. The signal yields in the $\psi(2S)$ and $\psi(3770)$ data are given in Table II.

The results for the ratio of branching ratios, R_J, for individual decay modes are given in Table III. Average values are calculated using inverse-of-statistical-errors-squared for weights. To estimate the statistical significance of $\psi(3770) \to \gamma\chi_{cJ}$ signals, we fit the $\psi(3770)$ data with the background contribution alone and compare the fit likelihoods to our nominal fits. Combining likelihoods for all the channels, we obtain statistical significance of $1.3, 3.6$ and 12.6 standard deviations for $J = 2$, 1 and 0, respectively. The sum of the photon spectra over the individual channels is shown for $\psi(2S)$ and $\psi(3770)$ data in Fig. 3. Since no significant signal is observed for $J = 2$, we set an upper limit for this state.

Various contributions to the systematic errors are listed in Table IV. We simulated signal events assuming various resonant substructures and compared the efficiency ratio to

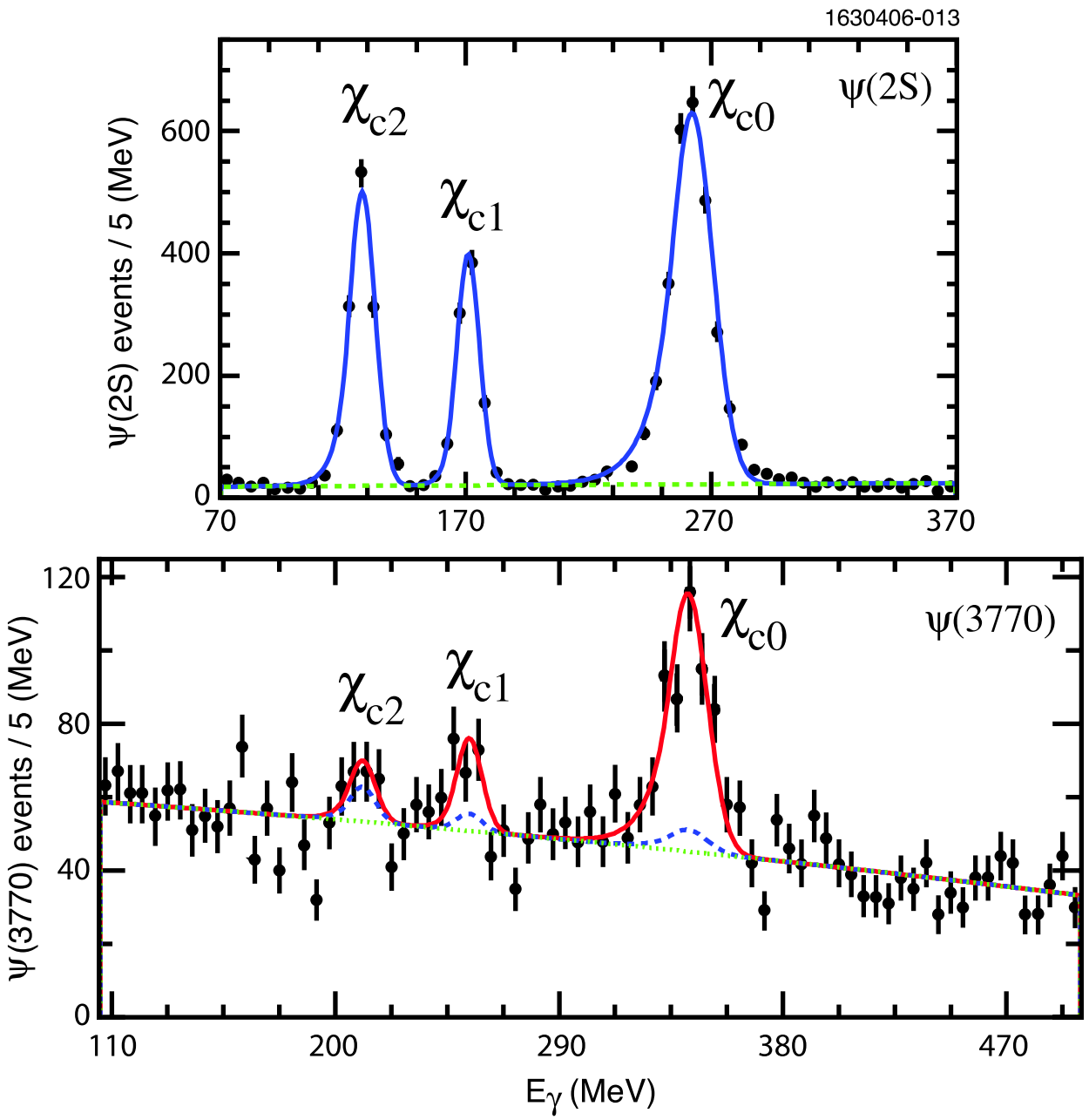

FIG. 3: Distribution of photon energy in CLEO-c $\psi(2S)$ (top) and $\psi(3770)$ (bottom) data summed over all analyzed modes (data points). The smooth curve shows the sum of the fits performed to the individual modes. The dashed curve shows the radiative tail from $\psi(2S)$. The dotted line shows the polynomial background.

our nominal values obtained with the phase-space model to evaluate the error in efficiency simulation. Including the systematic errors, our results for the ratio of branching ratios are: $R_0 = (7.9 \pm 0.8 \pm 0.6)\%$, $R_1 = (4.3 \pm 1.6 \pm 0.6)\%$ and $R_2 < 2.2\%$ (90% C.L.). The 3% uncertainty in the number of $\psi(2S)$ resonant decays contributes to the R_J measurement, but cancels when multiplied by the inclusively measured $\mathcal{B}(\psi(2S) \to \gamma\chi_{cJ})$ [10]. The results for $\mathcal{B}(\psi(3770) \to \gamma\chi_{cJ})$ are $(0.73 \pm 0.07 \pm 0.06)\%$, $(0.39 \pm 0.14 \pm 0.06)\%$ and $< 0.20\%$ (90% C.L.)

TABLE III: The ratio $R_J = \mathcal{B}(\psi(3770) \to \gamma\chi_{cJ}, \chi_{cJ} \to \pi^\pm, K^\pm)/\mathcal{B}(\psi(2S) \to \gamma\chi_{cJ}, \chi_{cJ} \to \pi^\pm, K^\pm)$. Only statistical errors are given here.

Decay mode	R_J in % $J=2$	$J=1$	$J=0$
4π	1.3 ± 1.5	3.8 ± 2.6	9.6 ± 1.4
$2K2\pi$	1.7 ± 2.4	9.9 ± 4.0	8.2 ± 1.7
6π	0.7 ± 1.8	2.9 ± 2.2	7.4 ± 1.8
$2K$	0.0 ± 1.4	–	6.0 ± 1.6
Average	0.8 ± 0.8	4.3 ± 1.6	7.9 ± 0.8

TABLE IV: Systematic errors and their sources.

	Relative change in % $J=2$	$J=1$	$J=0$
Luminosity	1	1	1
$\psi(3770)$ cross-section	3	3	3
Number of $\psi(2S)$ decays	3	3	3
Resonant substructure	2	< 1	< 1
$\pm 25\%$ change in $\psi(2S)$ bkg.	39	6	2
Fit systematics			
$\pm 7\%$ change in σ_E	10	8	4
$\pm 10\%$ change in fit range	17	5	1
Using Gaussian signal shape	9	2	1
Decreasing bin-size to half	15	3	< 1
± 1 order of bkg. polynomial	47	9	2
Total fit systematics	53	12	5
Total systematic error on R_J	66	14	7
$\mathcal{B}(\psi(2S) \to \gamma\chi_{cJ})$	6	5	4
Number of $\psi(2S)$ decays	-3	-3	-3
Total systematic error on $\mathcal{B}(\psi(3770) \to \gamma\chi_{cJ})$	66	15	8

for $J = 0, 1$ and 2, respectively. They are consistent with the results obtained previously by CLEO [5] using $\chi_{cJ} \to \gamma J/\psi$ decays: $< 4.4\%$ (90% C.L.), $(0.28 \pm 0.05 \pm 0.04)\%$ and $< 0.09\%$ (90% C.L.), correspondingly. The two analyses are complementary. While this analysis offers much better sensitivity for $J = 0$, the previous analysis is more sensitive for $J = 1$ and 2. The $J = 1$ signal is observed in both analyses. Combining both analyses we obtain $\mathcal{B}(\psi(3770) \to \gamma\chi_{c1}) = (0.29 \pm 0.05 \pm 0.04)\%$.

We turn the branching ratio results to transition widths using $\Gamma_{\rm tot} = (23.6 \pm 2.7)$ MeV from PDG [14]. The results are given in Table V, where they are compared to theoretical

TABLE V: Our measurements of the photon transitions widths (statistical and systematic errors) compared to theoretical predictions. The $J=0$ measurement comes from this analysis. The $J=2$ upper limit comes from Ref.[5]. The $J=1$ measurement comes from the combination of this analysis and of the result in Ref.[5].

	$\Gamma(\psi(3770)\to\gamma\chi_{cJ})$ in keV		
	$J=2$	$J=1$	$J=0$
Our results	<21	70 ± 17	172 ± 30
Rosner (non-relativistic) [7]	24 ± 4	73 ± 9	523 ± 12
Ding-Qin-Chao [6]			
non-relativistic	3.6	95	312
relativistic	3.0	72	199
Eichten-Lane-Quigg [8]			
non-relativistic	3.2	183	254
with coupled-channels corrections	3.9	59	225
Barnes-Godfrey-Swanson [9]			
non-relativistic	4.9	125	403
relativistic	3.3	77	213

predictions.

The theoretical predictions are based on potential model calculations [13] of the electric dipole matrix element $<1^3P_J|r|1^3D_1>$:

$$\Gamma_J = \frac{4}{3}e_Q^2\alpha E_\gamma^3 C_J <1^3P_J|r|1^3D_1>^2,$$

where e_Q is the c quark charge and α is the fine structure constant. The spin factors C_J are equal to 2/9, 1/6 and 1/90 for $J=0$, 1 and 2, respectively [15]. The phase-space factor (E_γ^3) also favors the $J=0$ transition. Together, the spin and phase-space factors predict enhancement of the $J=0$ width by a factor of ~ 3.2 and ~ 85 over $J=1$ and $J=2$, respectively. In the non-relativistic limit, the matrix element is independent of J. The measured ratios of the widths, $\Gamma_0/\Gamma_1 = 2.5\pm0.6$ and $\Gamma_0/\Gamma_2 > 8$ (90% C.L.), are consistent with these crude predictions, therefore, providing further evidence that $\psi(3770)$ is predominantly a 1^3D_1 state. A small admixture of 2^3S_1 wave, necessary to explain the observed $\Gamma_{ee}(\psi(3770))$, is expected to increase Γ_0 and Γ_2 while making Γ_1 smaller [6, 7]. The large experimental and theoretical uncertainties in Γ_J make testing of the mixing hypothesis via radiative transitions difficult.

As evident from Table V, the naive non-relativistic calculations tend to overestimate absolute values of the transition rates. Relativistic [6, 9] or coupled-channel [8] corrections are necessary for quantitative agreement with the data. The latter is not surprising since non-relativistic calculations also overestimate $\psi(2S)\to\gamma\chi_{cJ}$ transition rates [16].

We gratefully acknowledge the effort of the CESR staff in providing us with excellent luminosity and running conditions. This work was supported by the A.P. Sloan Foundation, the National Science Foundation, the U.S. Department of Energy, and the Natural Sciences

and Engineering Research Council of Canada.

---

[1] Belle Collaboration, S. K. Choi *et al.*, Phys. Rev. Lett. **91**, 262001 (2003); BABAR Collaboration, B. Aubert *et al.*, Phys. Rev. D**73**, 011101(R) (2006); CLEO Collaboration, T. E. Coan *et al.*, Phys. Rev. Lett. **96**, 162003 (2006).

[2] T. Appelquist, A. de Rujula, H. D. Politzer, Phys. Rev. Lett. **34**, 43 (1975); C. G. Callan, R. L. Kingsley, S. B. Treiman, F. Wilczek, A. Zee, Phys. Rev. Lett. **34**, 52 (1975); T. Appelquist, A. de Rujula, H. D. Politzer, Phys. Rev. Lett. **34**, 365 (1975); E. Eichten, K. Gottfried, T. Kinoshita, J. Kogut, K. D. Lane, T.-M. Yan, Phys. Rev. Lett. **34**, 369 (1975).

[3] BES Collaboration, J.Z. Bai *et al.*, Phys. Lett. B**605**, 63 (2005).

[4] CLEO Collaboration, N.E. Adam *et al.*, Phys. Rev. Lett. **96**, 082004 (2006).

[5] CLEO Collaboration, T. E. Coan *et al.*, Phys. Rev. Lett. **96**, 182002 (2006), arXiv:hep-ex/0509030.

[6] Y.-B. Ding, D.-H. Qin, K.-T. Chao, Phys. Rev. D **44**, 3562 (1991).

[7] J. L. Rosner, Phys. Rev. D**64**, 094002 (2001); J. L. Rosner, Annals Phys. **319**, 1 (2005), arXiv:hep-ph/0411003.

[8] E. J. Eichten, K. Lane and C. Quigg, Phys. Rev. D**69**, 094019 (2004).

[9] T. Barnes, S. Godfrey and E. S. Swanson, Phys. Rev. D **72**, 054026 (2005), arXiv:hep-ph/0505002.

[10] CLEO Collaboration, S. B. Athar *et al.*, Phys. Rev. D**70**, 112002 (2004).

[11] CLEO Collaboration, Y. Kubota *et al.*, Nucl. Instrum. Methods Phys. Res., A**320**, 66 (1992); D. Peterson *et al.*, Nucl. Instrum. Methods Phys. Res., A**478**, 142 (2002); M. Artuso *et al.*, Nucl. Instrum. Methods Phys. Res., A**554** 147 (2005).

[12] R. Brun *et al.*, GEANT 3.21, CERN Program Library Long Writeup W5013 (1993), unpublished.

[13] See e.g. Eq. (4.118) in N. Brambilla *et al.*, arXiv:hep-ph/0412158 (unpublished).

[14] Particle Data Group, S. Eidelman *et al.*, Phys. Lett. B **592**, 1 (2004).

[15] See e.g., W. Kwong and J. L. Rosner, Phys. Rev. D **38**, 279 (1988).

[16] T. Skwarnicki, Int. J. Mod. Phys. A **19**, 1030 (2004).